AIP Journal of Applied Physics

Enhanced visible fluorescence in highly transparent Al-doped ZnO film by surface plasmon coupling of Ag nanoparticles

Swati Bishnoi, Rupali Das, Parikshit Phadke, R. K. Kotnala, and Santa Chawla

Citation: Journal of Applied Physics **116**, 164318 (2014); doi: 10.1063/1.4900733

View online: http://dx.doi.org/10.1063/1.4900733

View Table of Contents: http://scitation.aip.org/content/aip/journal/jap/116/16?ver=pdfcov

Published by the AIP Publishing

Enhanced visible fluorescence in highly transparent Al-doped ZnO film by surface plasmon coupling of Ag nanoparticles

Swati Bishnoi, Rupali Das, Parikshit Phadke, R. K. Kotnala, and Santa Chawla[a)]
CSIR-National Physical Laboratory, Dr. K. S. Krishnan Road, New Delhi 110012, India

(Received 5 June 2014; accepted 16 October 2014; published online 31 October 2014)

ZnO:Al (AZO) film has been deposited on quartz substrate by Pulsed laser deposition and showed monophasic hexagonal structure of c-axis oriented nanorods upto 80 nm in height. AZO film was optimally conjugated with Ag nanoparticles (Ag NPs) in a hybrid nanostructure to achieve significant enhancement in the visible fluorescence emission. Augmented near field and extinction spectra of shape tailored Ag NPs and their dimers are simulated through FDTD method, and a direct association with fluorescence enhancement is established. Such plasmon- enhanced visible emission from a transparent conducting oxide could be very important for solar cell applications. © *2014 AIP Publishing LLC*. [http://dx.doi.org/10.1063/1.4900733]

I. INTRODUCTION

Recently, Aluminum doped zinc oxide (AZO) materials have attracted much interest due to their wide applications like fabrication of various types of devices, in optoelectronics such as optical sensors, light emitters,[1,2] blue light emitting diodes (LEDs),[3] lasers, and phosphors because of their interesting magnetic[4] and optical properties.[5,6] In addition to having excellent optical and electronic properties, AZO offers the advantage of being a lower cost, lesser toxicity material abundant compared to the other widely used transparent conducting oxide (TCO), e.g., indium tin oxide (ITO).[7] At the same time, TCO nanocrystals (NCs) are of renewed interest as exploiting size-dependent properties in them is easy.[8,9] Among TCO materials, AZO is a special material due to multifunctional properties of ZnO such as UV and visible emission, piezoelectric and ferroelectric behaviour, and dilute ferromagnetism with appropriate doping. AZO shows conductivity enhancement as compared to undoped ZnO along with improved transparency,[10,11] hence can act as a potential candidate to be a substitute for indium-tin-oxide (ITO) materials.[12] AZO film also has a potential application in silicon solar cell as surface passivation and anti-reflection layer. ZnO being an excellent emitter under UV excitation (band gap 3.3 eV), AZO also exhibits fluorescence. With enhanced fluorescence from AZO mediated by plasmonic near field, AZO film can serve dual purpose of solar spectrum converter from UV to visible for improvement in light conversion efficiency of solar cells.

In recent years, optical properties of metal nanoparticles and plasmon enhanced fluorescence have been widely investigated.[13–15] Surface plasmon resonance (SPR) of metal nanoparticles leads to significant enhancement of local electromagnetic (EM) field intensity which could result in increased optical response from fluorophores. Improvement in optical and other properties of AZO film have been reported while conjugated with metal nanoparticles (MNP).[16,17] By introducing silver nanoparticles (AgNPs) inside AZO film, light harvesting was enhanced because of plasmonic light scattering effects.[18] Almost all studies in AZO film deals with electronic and optical transmission characteristics,[10,11] but the important attribute of fluorescence from AZO film is rarely reported. Moreover, reports on fluorescence emission from ZnO and its conjugation with metal nanoparticles (MNP) are mostly concerned about UV emission. As visible emission from a TCO materials could be of utmost importance for optoelectronic as well as solar cell applications, in this article, we are reporting deposition of thin transparent layer of AZO by pulsed laser deposition and significant enhancement in visible fluorescence when optimally coupled with shape tailored silver nanoparticles. To avoid fluorescence quenching due to direct contact between AZO nanoparticles and Ag NPs, a spacer layer in the form of linker molecule such as PVA is used.[19–21]

II. EXPERIMENTAL PROCEDURES

A. Synthesis of ZnO:Al and thin film deposition

For the synthesis of Al (5%) doped ZnO nanocrystals, analytical grade commercial zinc oxide ZnO (99.99% Pure) and aluminum oxide Al_2O_3 (99.99% Pure) have been used. Al doped ZnO nanoparticles are synthesized by controlled reaction in the solid state. The precursor materials were mixed thoroughly and fired at 1200 °C for 2 h in air atmosphere. The resulting product was cooled slowly and grinded. The synthesized ZnO:Al powder was characterized by XRD[33] and found to be highly crystalline in monophasic hexagonal wurtzite structure and showed photoluminescence (PL) excitation in UV region.[33] A pellet was made with the synthesized AZO powder and sintered at 1200 °C. This sintered pellet was used as a target for film deposition on quartz substrate by pulsed laser deposition using KrF laser (248 nm Excel Chamber, energy 400 mJ, frequency 5 Hz). The deposition was carried out in oxygen atmosphere

[a)]Author to whom cporrespondence should be addressed. Electronic mail: santa@nplindia.org

(O_2 pressure—1 × 10^{-2}Torr) by maintaining the quartz substrate temperature at 700 °C.

B. Synthesis of Ag nanoparticles and integration with AZO film

The Ag NP colloidal solution with average particle size 50 nm was synthesized by adopting the method developed by metraux and mirkin[22] and their morphology was studied by TEM. Confocal fluorescence mapping and spectroscopy were done on the AZO film on Quartz. To investigate the plasmonic effect on the same area of AZO film—without disturbing the AZO film position on the microscope platform, first, a spacer layer of PVA (3% PVA in water) of few nm thickness was deposited on AZO Pulsed laser deposition (PLD) film and then the blue colloidal silver solution was drop casted on the top of this PVA spacer layer separating the AZO layer and Ag nanoparticles.

C. Characterization

The X-ray powder diffraction (XRD) of the deposited PLD film of AZO on quartz were examined on a Rigaku miniflex X-ray diffractometer using the principle of Bragg Brentano Geometry, with Cu-Kα radiation (1.54 A°). The morphology of the AZO film was studied by Atomic Force Microscope (NT-MDT Model #- BL022SMT). The thickness of the AZO film was measured by Stylus Profilometer (Ambios XP200) and varied between 50 to 80 nm in different points. The absorption spectra of the Ag NP solution and transparency of AZO film were measured using Avantes UV-Visible spectrometer. The photoluminescence (PL) characteristics were studied under a WITec Confocal fluorescence microscope (WITec 300M^{+}) with PL mapping facility. A specific area of the film was chosen under a 20× objective in the confocal microscope and fluorescence distribution was recorded under UV (375 nm) excitation of the as deposited AZO film and AZO film-PVA-Ag NP hybrid structure. Time resolved photoluminescence (PL) decay was measured using Edinburgh Instruments Time resolved spectrometer (FLSP920) using a pulsed Xe lamp as excitation source and employing time correlated single photon counting (TCSPC) technique.

III. RESULTS AND DISCUSSION

A. XRD, AFM, and HRTEM

The XRD and AFM images of the sample are shown in Figure 1. The XRD spectra (Fig. 1(a)) of AZO film show two peaks mainly (100) of silica substrate and (002) of AZO film, the presence of only (002) peak suggests formation of c-axis oriented rods. The transmission spectra of the film show more than 80% transmittance in the visible region. The 2D AFM image (Fig. 1(b)) indicates near uniform density of AZO particles over the substrate and 3D image (Fig. 1(c)) clearly reveals elongated rod type particles (upto 80 nm height). The TEM images of representative Ag particles are shown in Fig. 1(d), and the schematic diagram of the hybrid system comprising AZO film-PVA spacer layer-Ag NP layers is shown in Fig. 1(e); the light was incident perpendicularly to the film surface in confocal fluorescence measurement setup.

B. Fluorescence enhancement and time resolved decay

The optical and corresponding confocal fluorescence images of AZO film without and with Ag NPs are shown in Figs. 2(a) and 2(d); 2(b) and 2(e), respectively. The corresponding integrated PL emission spectra of exactly the same area of the film under 375 nm light excitation are shown in

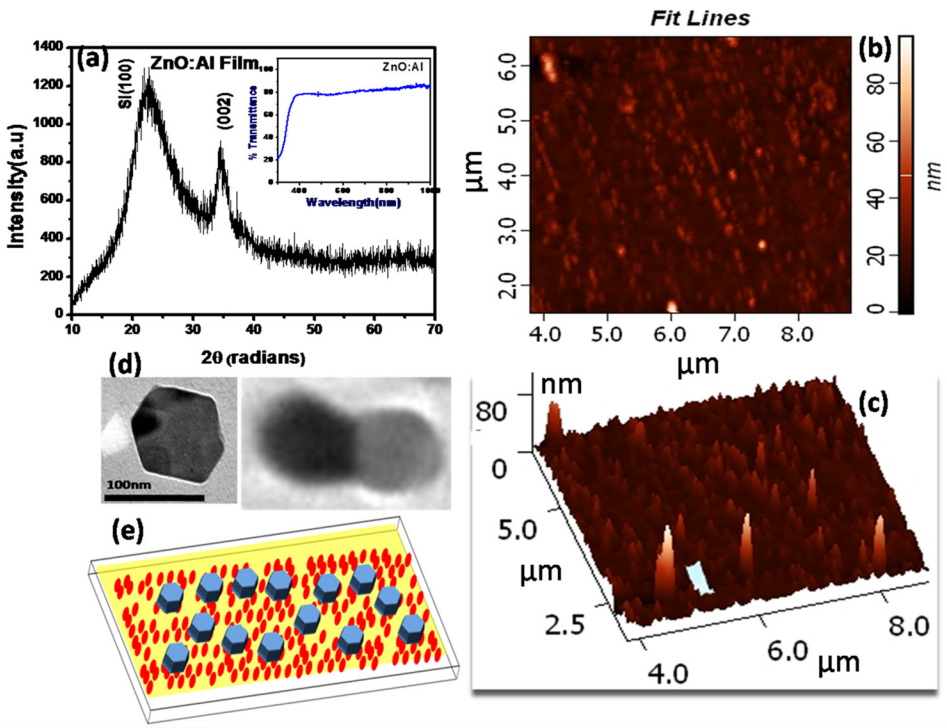

FIG. 1. (a) XRD spectra of AZO PLD film on quartz substrate, inset shows optical transmission spectra; AFM image (b) (2D) and (c) 3D of AZO film; (d) Representative TEM images of Ag NPs and (e) schematic of arrangements of ZnO:Al (red spheres), PVA layer (yellow transparent layer) and Ag NPs (blue hexagons) used for confocal fluorescence study.

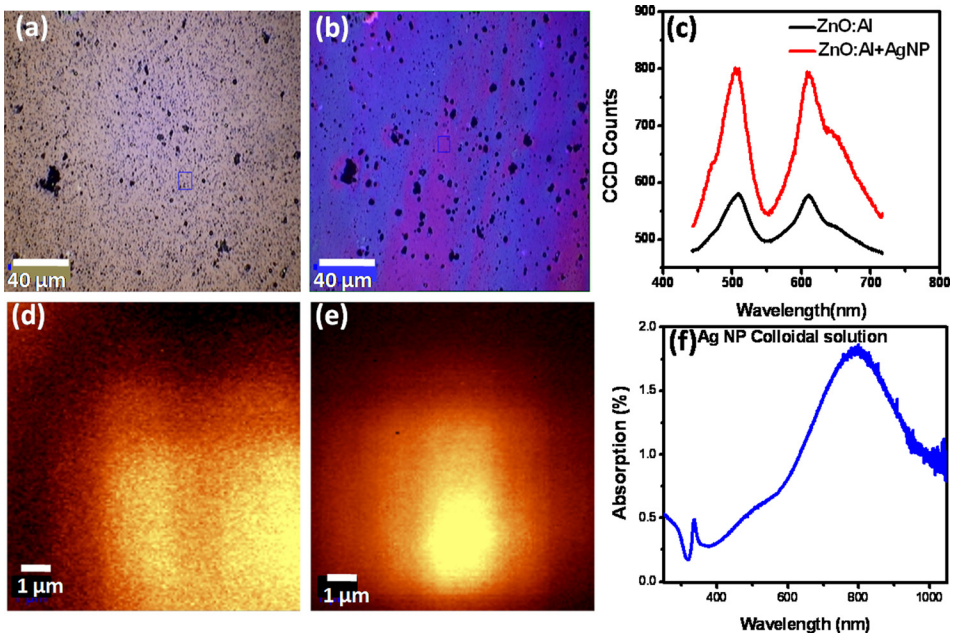

FIG. 2. (a) Optical image of AZO (b) AZO + Ag NP film (d) and (e) corresponding confocal fluorescence image of AZO & AZO + Ag NP film (c) confocal fluorescence spectra (integrated) under 375 nm laser excitation with and without Ag NP (f) measured absorption spectra of Ag nanoparticles.

Fig. 2(c) and clearly reveal fluorescence enhancement of 2.9 times for the green (508 nm peak) and 3.2 times for the orange (611 nm peak) emission. The confocal fluorescence maps of the selected area of AZO film without (Fig. 2(d)) and with Ag NPs (Fig. 2(e)) show the region of intense fluorescence due to presence of Ag NPs. The observed emission enhancement could be attributed to the plasmonic near field mediated effect of the Ag NPs in proximity to the AZO nanorods grown on the quartz substrate. The UV-Visible absorption spectra of Ag NP colloidal solution (Fig. 2(f)) exhibits a sharp out of plane quadrupolar resonance peak at 335 nm, a broad in plane quadrupolar resonance around 500 nm[23] and a broad dipolar peak centered at 795 nm. The absorption spectra of Ag NPs cover the emission and also excitation range of ZnO:Al.[33] It has been reported that metal enhanced fluorescence, when the fluorophore is in close proximity to silver nanoparticles, can be realized when the distance between the metal particle and the fluorophore is from about 4 nm to about 2000 nm, preferably from about 40 nm to about 200 nm.[24] Fluorescence enhancement variation with oxide spacer layer thickness ranging from 0 to 440 nm, with maximum enhancement obtained around 70 nm spacer layer,[25] enhanced photoluminescence and external quantum yield from 7% to 42% from J-aggregate film followed by a 100 nm thick spin-coated PVA layer[26] have been observed. In our case, typical thickness of PVA spacer layer is about 100 nm, as measured by optical profilometry [Stylus Profilometer (Ambios XP200)]. Moreover, in studies of fluorescence nanoparticle conjugation with Ag NPs, we have done a systematic study of PVA concentration and layer deposition parameters and found that in most inorganic nanopartcles and Ag NP combination, the spacer layer thickness as employed in the present case produce best results.[27,28]

Metal enhanced fluorescence (MEF) can occur either through excitation enhancement (enhancement of local EM field) and/or through emission enhancement (enhancement of radiative decay rate). However, to distinguish between these two components is not an easy task, particularly when broad SPR band of Ag NPs (Fig. 2(f)) overlap with both excitation and emission spectrum of the AZO nanoparticles. Excitation enhancement produces a higher excitation rate but does not change the decay time of the fluorophore. On the other hand, emission enhancement increases the radiative decay rate, thus shortening the luminescence decay time.[29] In our case, when Ag NPs are conjugated with AZO film, the green emission enhances 2.9 times and red emission by 3.2 times compared to only AZO film.

In order to understand the excitation and emission enhancement process in relation to the SPR spectrum of Ag NPs for green and red emission of AZO film, we have measured time resolved decay of both green and red emission from AZO film and AZO film – Ag NP integrated system under excitation of a 375 nm pulsed source. The luminescence decay plots are shown in (Fig. 3) and clearly display the varied effect on decay process of green and red emission due to proximity of Ag NPs. The decay curves (Fig. 3) clearly show that decay characteristics for green emission remain almost similar with and without Ag NPs. This suggests that prominent mechanism for green emission enhancement would be through enhancement of near field due to presence of Ag NPs in proximity. On the other hand, for red emission, decay curves (Fig. 3) unambiguously show a faster decay after Ag NP conjugation. These decay characteristics suggest more prominent role of emission enhancement for red emission. Weak coupling of green emission line with the in plane quadrupolar resonance (~500 nm) and stronger coupling of red emission with the dipolar peak results in such decay characteristics.

The proximity of Ag NPs with the AZO film greatly enhances the visible emission through coupling of plasmonic modes in their near field regions. The Ag particles when excited by an incident EM field have the striking ability to design their localized field through SPR tuning and lightning rod effect. The near field generated by the metal nanoparticles (MNP) could increase the fluorescence by excitation or emission enhancement for which the excitation or emission

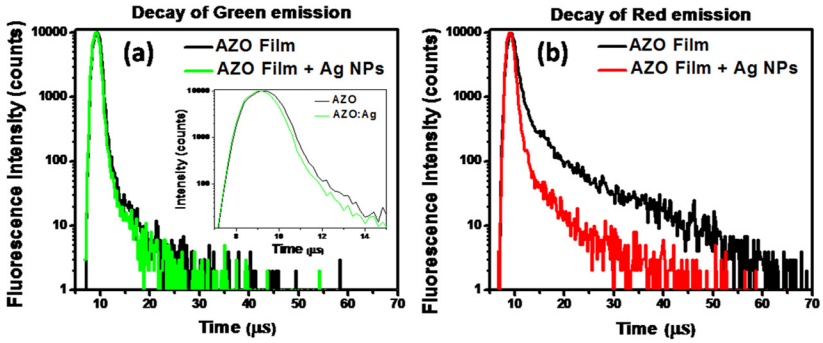

FIG. 3. Time resolved decay of luminescence of both (a) green emission (inset shows magnified scale) and (b) red emission of AZO film and AZO + Ag NP combine.

spectra of the fluorophore must overlap with the SPR of MNPs.[27] The bound excitons of the ZnO nanoparticles can couple to the coherent oscillations of the surface plasmons that lead to augmented local field over the incident electromagnetic field.

C. Finite difference time domain (FDTD) simulation

To comprehend the magnitude of such local field enhancements around Ag NPs under exciting UV light, FDTD simulation method (version 8.7.1)[30] was employed to generate near field of exact Ag NPs and their dimers. The FDTD technique employs the solution of Maxwell's electromagnetic equation considering both the E(t) and H(t) components discrete over time to obtain steady-state continuous wavefield E(ω) by Fourier transformation of E(t) for plasmonic structures with complex geometries. One exact Ag NP (nanohexagon, imported from TEM micrograph, Fig. 4(a)), from the solution was considered on average geometrical distribution for the simulation. Mesh size 0.8 nm was used for higher degree of accuracy. The material response was taken from Palik[31,33] (0–2 μm) and the field was allowed to evolve for 200 fs. The light was incident along Z-axis, perpendicular to Ag NP surface, akin to confocal fluorescence measurements. The simulated near field results of single Ag nanohexagon (Fig. 4(b)) and dimer (Fig. 4(c)) clearly elucidate the near field generated around the nanoparticle and the effect of addition of Ag NPs in a dimer formation in a linear array with interparticle separation of 5 nm. At 375 nm incident wavelength, the calculated $|E|^2/|E_0|^2$ value for the hexagonal Ag NP reaches 19 times the incident field. The augmented near field significantly confines the incoming electromagnetic radiation leading to crowded electric lines generating hot spots due to the generated modes of SPR and the lightening rod effect in the Ag nanoheaxagon (Fig. 4(b)). The field enhancement increases 63 times the incident field (3.3 times that of a single Ag nanohexagon) for dimer (Fig. 4(c)) due to confinement of field in the intergap region of Ag NPs as well as around them. Larger enhancements are expected for larger ensembles of particles. This plasmonic near field contribute effectively to the fluorescence enhancement process in the

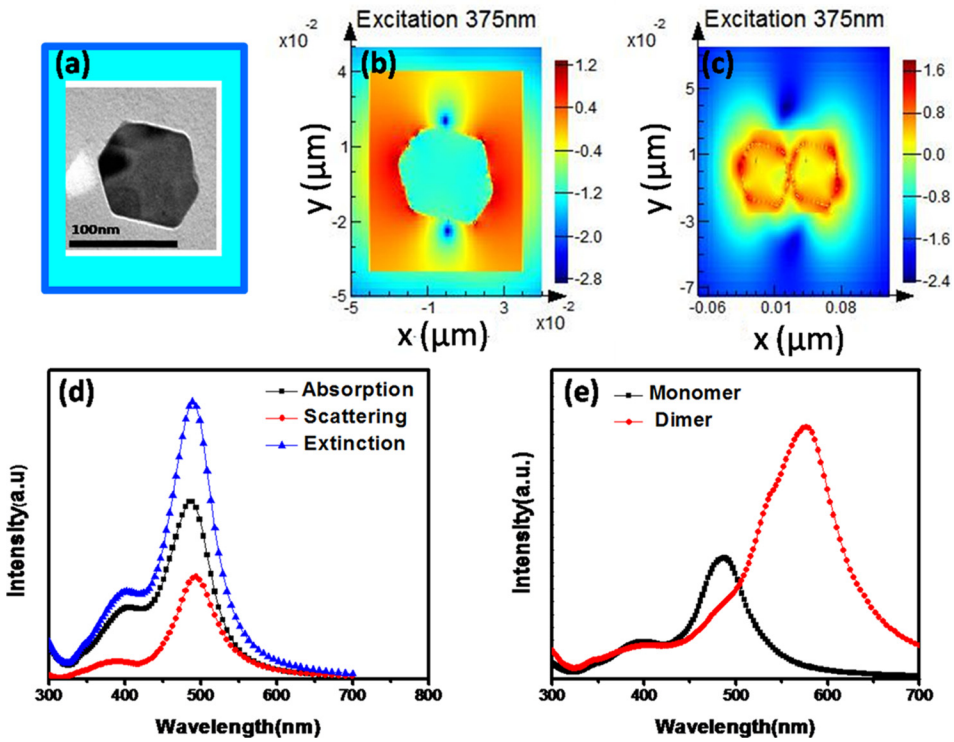

FIG. 4. (a) TEM image of Ag NP; FDTD simulated (b) near field ($|E|^2$) of single Ag nanohexagon (monomer, dimension (~50 nm)) and (c) dimer, log scale is depicted, (d) absorption, scattering, and extinction spectra of a monomer and (e) extinction spectra of monomer and dimer.

integrated Ag NP-AZO hybrid system. Thus, the proximity of Ag NPs optimally integrated with AZO PLD film leads to the observed fluorescence enhancements in the hybrid system to significant degrees through plasmonic coupling of LSPRs and near field mediated excitation enhancement.

To further elucidate the effect of SPR of Ag NP and their hybrids on the fluorescence enhancement of AZO, single particle absorption, scattering, and extinction spectra have been simulated (Fig. 4). The simulated spectra clearly show that scattering component which mainly contributes towards emission enhancement is appreciable. Going from single particle to dimer, the extinction broadens and red shifts (Fig. 4(d)). In the experimental AZO-Ag NP integrated thin film system, there would be many Ag NP hybrids near AZO particles, hence overlapping of SPR band and red emission band of AZO would happen leading to fluorescence enhancement. Therefore, both excitation and emission enhancement are likely to have contributed to the MEF process of Ag NP conjugated AZO film. Such partial contribution of excitation and emission enhancement of green and red upconversion emission has also been reported.[29,32]

IV. CONCLUSION

In summary, we have deposited AZO film on quartz substrate in oxygen atmosphere with monophasic hexagonal structure of c-axis oriented nanorods upto 80 nm in height. The film thickness and particle morphology have been confirmed through profilometry and AFM studies. The deposited film has more than 80% transparency in the visible region. Optimal conjugation of AZO film with Ag NPs separated by a polymer (PVA) layer lead to fluorescence enhancement in the visible region as observed in confocal fluorescence spectroscopy and imaging. The near field generated around Ag nanoparticles and their aggregates under UV excitation play a key role in enhancing the fluorescence emission of AZO particles. A consolidated study of fluorescence, time resolved decay of green and red emission, UV-Visible absorption of Ag NP colloidal solution used for conjugation with AZO film, FDTD simulation of near field and extinction spectra of Ag NPs and their hybrids clearly suggest that both excitation and emission enhancement contribute to the MEF process of Ag conjugated AZO film. Whereas, the improvement in green fluorescence is mainly through excitation enhancement, the augment in red fluorescence is through emission enhancement process. Such cases of conjugation of AZO film with Ag NPs leading to enhanced intensity, while simultaneously shortening the fluorescence lifetime, open up possibilities of obtaining significantly augmented fluorescence emission with decreased excitation intensity.

ACKNOWLEDGMENTS

This present work was supported by the TAPSUN project under CSIR Solar Mission program of India.

[1]J. Nayak, S. Kimura, S. Nozaki, H. Ono, and K. Uchida, Superlatt. Microstruct. **42**, 438 (2007).
[2]Q. Xiang, G. Meng, Y. Zhang, J. Xu, P. Xu, Q. Pan, and W. Yu, Sens. Actuators, B **143**, 635 (2010).
[3]M. H. Huang, S. Mao, H. Feick, H. Q. Yan, Y. Y. Wu, H. Kind, E. Weber, R. Russo, and P. D. Yang, Science **292**, 1897 (2001).
[4]X. Huang, G. Li, B. Cao, M. Wang, and C. Hao, J. Phys. Chem. C. **113**, 4381–4385 (2009).
[5]G. Murugadoss, J. Lumin. **132**, 2043 (2012).
[6]K. M. K. Srivatsa, D. Chhikara, and M. Senthil Kumar, J. Mater. Sci. Technol. **27**, 701 (2011).
[7]Minami, T. Semicond. Sci. Technol. **20**, S35–S44 (2005).
[8]T. Thu and V. S. Maenosono, J. Appl. Phys. **107**, 014308 (2010).
[9]K. J. Chen, T. H. Fang, F. Y. Hung, L. W. Ji, S. J. Chang, S. J. Young, and Y. J. Hsiao, Appl. Surf. Sci. **254**, 5791(2008).
[10]Z. Y. Ning, S. H. Cheng, S. B. Ge, Y. Chao, Z. Q. Gang, Y. X. Zhang, and Z. G. Liu, Thin Solid Films **307**, 50(1997).
[11]K. Postava, H. Sueki, M. Aoyama, T. Yamaguchi, K. Murakami, and Y. Igasaki, Appl. Surf. Sci. **175/176**, 543 (2001).
[12]M. Chen, Z. L. Pei, C. Sun, L. S. Wen, and W. J. Wang, Cryst. Growth **220**(3), 254(2000).
[13]K. Ishkawa and T. Okudo, J. Appl. Phys. **98**, 043502 (2005).
[14]S. K. Lim, K. J. Chung, and C. K. Kim, J. Appl. Phys. **98**, 084309 (2005).
[15]U. Hohenester and J. Krenn, Phys. Rev. B **72**, 195429 (2005).
[16]A. V. Zayats and I. I. Smolyaninov, J. Opt. A **5**, S16 (2003).
[17]G. Laurent, N. Felidj, and J. Aubard, J. Chem. Phys. **122**, 011102 (2005).
[18]J. Yun, E. Kozarsky, J. Kim, H. S. Kojori, S. J. Kim, C. Tong, J. Wang, and W. A. Anderson, *IEEE Photovoltaics Specialists Conference* (IEEE, 2011).
[19]Q. Wang, F. Song, S. Lin, J. Liu, H. Zhao, C. Zhang, C. Ming, and E. Y. B. Pun, Opt. Express **19**, 6999–7006 (2011).
[20]W. Feng, L. D. Sun, and C. H. Yan, Chem. Commun. **29**, 4393 (2009).
[21]P. Anger, P. Bhardwaj, and L. Novotny, Phys. Rev. Lett. **96**, 113002 (2006).
[22]G. S. Meutrax and C. A. Mirkin, Adv. Mater. **17**(4), 412 (2005).
[23]K. L. Kelly, E. Coronado, L. L. Zhao, and G. C. Schatz, J. Phys. Chem. B **107**, 668–677 (2003).
[24]C. D. Geddes, U.S. patent No. US 20,130,102,770 A9 (25 April, 2013).
[25]S.-H. Guo, D. G. Britti, J. J. Heetderks, H.-C. Kan, and R. J. Phaneuf, Nano Lett. **9**, 2666 (2009).
[26]G. M. Akselrod, Y. R. Tischler, E. R. Young, D. G. Nocera, and V. Bulovic, Phys. Rev. B **82**, 113106 (2010).
[27]Z. Buch, V. Kumar, H. Mamgain, and S. Chawla, Chem. Comun. **49**, 9485 (2013).
[28]Z. Buch, V. Kumar, H. Mamgain, and S. Chawla, J. Phys. Chem. Lett. **4**, 3834 (2013).
[29]W. Deng, L. Sudheendra, J. K. Zhao, J. Fu, D. Jin, I. M. Kennedy, and E. M. Goldys, Nanotechnology **22**, 325604 (2011).
[30]Reference Guide for FDTD Solutions, available at: www.lumerical.com/fdtd, 2013.
[31]E. D. Palik, *Handbook of Optical Constants of Solids* (Academic Press, New York, 1985).
[32]K. Li, M. I. Stockman, and D. J. Bergman, Phys. Rev. B **72**, 153401 (2005).
[33]See supplementary material at http://dx.doi.org/10.1063/1.4900733 for PLE and XRD spectra of AZO and FDTD Simulation Parameter.